PROCEEDINGS OF SPIE

SPIEDigitalLibrary.org/conference-proceedings-of-spie

In vitro terahertz spectroscopy of gelatin-embedded human brain tumors: a pilot study

N. V. Chernomyrdin, A. A. Gavdush, S.-I. T. Beshplav, K. M. Malakhov, A. S. Kucheryavenko, et al.

N. V. Chernomyrdin, A. A. Gavdush, S.-I. T. Beshplav, K. M. Malakhov, A. S. Kucheryavenko, G. M. Katyba, I. N. Dolganova, S. A. Goryaynov, V. E. Karasik, I. E. Spektor, V. N. Kurlov, S. O. Yurchenko, G. A. Komandin, A. A. Potapov, V. V. Tuchin, K. I. Zaytsev, "In vitro terahertz spectroscopy of gelatin-embedded human brain tumors: a pilot study," Proc. SPIE 10716, Saratov Fall Meeting 2017: Optical Technologies in Biophysics and Medicine XIX, 107160S (26 April 2018); doi: 10.1117/12.2316302

SPIE.

Event: Saratov Fall Meeting 2017, 2017, Saratov, Russian Federation

In vitro terahertz spectroscopy of gelatin-embedded human brain tumors – a pilot study

N.V. Chernomyrdin[a,b,c], A.A. Gavdush[a], S.-I.T. Beshplav[d], K.M. Malakhov[a], A.S. Kucheryavenko[a], G.M. Katyba[e], I.N. Dolganova[a], S.A. Goryaynov[d], V.E. Karasik[a], I.E. Spektor[b], V.N. Kurlov[e], S.O. Yurchenko[a], G.A. Komandin[b], A.A. Potapov[d], V.V. Tuchin[f,g,h], and K.I. Zaytsev[a,b,c]

[a]Bauman Moscow State Technical University, Moscow 105005, Russia
[b]Prokhorov General Physics Institute of RAS, Moscow 119991, Russia
[c]Sechenov First Moscow State Medical University, Moscow 119991, Russia
[d]Burdenko Neurosurgery Institute, Moscow 125047, Russia
[e]Institute of Solid State Physics of RAS, Chernogolovka 142432, Russia
[f]Saratov State University, Saratov 410012, Russia
[g]Institute of Precision Mechanics and Control of RAS, Saratov 410028, Russia
[h]Tomsk State University, Tomsk 634050, Russia

ABSTRACT

We have performed the *in vitro* terahertz (THz) spectroscopy of human brain tumors. In order to fix tissues for the THz measurements, we have applied the gelatin embedding. It allows for preserving tissues from hydration/dehydration and sustaining their THz response similar to that of the freshly-excised tissues for a long time after resection. We have assembled an experimental setup for the reflection-mode measurements of human brain tissues based on the THz pulsed spectrometer. We have used this setup to study *in vitro* the refractive index and the amplitude absorption coefficient of 2 samples of malignant glioma (grade IV), 1 sample of meningioma (grade I), and samples of intact tissues. We have observed significant differences between the THz responses of normal and pathological tissues of the brain. The results of this paper highlight the potential of the THz technology in the intraoperative neurodiagnosis of tumors relying on the endogenous labels of tumorous tissues.

Keywords: terahertz radiation, terahertz pulsed spectroscopy, human brain tumor, malignant glioma, meningioma, intraoperative diagnosis, gelatin embedding.

1. INTRODUCTION

During the past decades, a considerable progress in the terahertz (THz) science and technology has been observed.[1,2] Methods of THz spectroscopy and imaging have been applied for solving numerous fundamental and applied problems in condensed matter physics,[3–6] gas sensing,[7] chemical and pharmaceutical sciences,[8,9] non-destructive testing,[10,11] security tasks,[10,12,13] etc. Among all these applications, the use of THz technology in medical diagnosis of malignancies attracts a special attention[14,15] due to both non-invasiveness of the low-power THz radiation[16] and intrinsic character of contrast, which is primarily due to the increased water content in malignant tissues as a result of their abnormal vascularity and edema.[17–19] In particular, these differences yield the non-invasive diagnosis of skin cancers,[20–24] the least-invasive diagnosis of oral, liver, gastric and colon cancers,[25–31] and the intraoperative monitoring of breast tumor resection.[32–36] Rapid progress in biomedical applications of THz science and technologies pushes further research in the area of THz medical diagnosis into the realm of studying malignancies in various localizations of human body, analyzing the origins of differences observed between the normal and malignant tissues, and, finally, developing novel instruments of

Further author information:
Nikita V. Chernomyrdin, E-mail: chernik-a@yandex.ru;
Kirill I. Zaytsev, E-mail: kirzay@gmail.com

Saratov Fall Meeting 2017: Optical Technologies in Biophysics and Medicine XIX, edited by Elina A. Genina, Irina Yu. Goryacheva. Valery V. Tuchin, Proc. of SPIE Vol. 10716, 107160S

the THz spectroscopy and imaging, which are portable, ergonomic, fast, and, thus, reliable for use in a clinical practice.[37,38]

Recently, a remarkable results in the area of the THz medical diagnosis has been reported – i.e. an ability for discriminating malignant brain gliomas from healthy (intact) tissues has been demonstrated highlighting the prospectives of the THz technology in the intraoperative neurodiagnosis.[39–42] The *in vitro* THz dielectric spectroscopy of paraffin-embedded brain glioma of mouse model has shown significant contrast between the THz responses of healthy and abnormal tissues – the paraffin-embedded glioma possesses higher refractive index and absorption coefficient.[39] Furthermore, the reflection-mode imaging of brain gliomas of the rat models *in vitro* and *in vivo* and human brain *in vitro* at the frequency of 0.5 THz demonstrates an ability for accurate detection of the tumor margins.[42] Nevertheless, the development of novel instruments for the THz intraoperative diagnosis of brain tumors still remains challenging owing to the absence of verified database of the THz dielectric characteristics of normal and pathological tissues, which needs large amount of samples to be measured either *in vivo* or *ex vivo* and allows to estimate sensitivity and specificity of the THz diagnosis, as well as to the absence of the THz instruments reliable for use in a clinical environment.

In this paper, we perform the *in vitro* terahertz (THz) spectroscopy of human brain tumors – 2 samples of malignant glioma (grade IV), 1 sample of meningioma (grade I), and samples of healthy (intact) tissues. To preserve brain tissues for the THz measurements, we use gelatin embedding,[43] which allows for minimizing hydration/dehydration of tissues during transportation and measurements, and sustaining the response of tissues at THz frequencies similar to that of the freshly-excised ones. We assemble an experimental setup for the reflection-mode measurements of human brain tissues based on the THz pulsed spectrometer. We apply it for studying *in vitro* the refractive index and the amplitude absorption coefficient of tissues in the frequency range from 0.05 to 1.1 THz. We demonstrate the increased THz refractive index and absorption coefficient of the gelatin-embedded tumor tissues compared to the intact ones, which originates owing to the endogenous features of tissues.[44–47] The observed differences between the THz characteristics of normal and pathological tissues highlight the potential of the THz spectroscopy and imaging in the intraoperative neurodiagnosis – i.e. they could be applied for the intraoperative detection of the tumor margins in order to guarantee the gross total resection of the tumor.

2. MATERIALS AND METHODS

2.1 Gelatin-embedded human brain tissues

As shown in Tab. 1, in this work, we measured *in vitro* healthy (intact) tissues and tumors of the brain – i.e. 2 samples of malignant glioma (grade IV) and 1 sample of meningioma (grade I). These samples were investigated no later than 4 hours after the surgical resection performed according to the medical recommendations in Burdenko Neurosurgery Institute (Moscow, Russia). The neurosurgery of tumors was assisted by the intraoperative exogenous fluorescence imaging, relying on the fluorescence of protoporphyrin IX (PpIX), which is induced by 5-aminolevulinic acid (5-ALA) and yields determining the tumor margins.[48–51] We should notice that only one of the two measured gliomas effectively accumulated the PpIX during the neurosurgery providing an ability for the intraoperative fluorescence diagnosis. Thus, a comparison of the THz responses of these two different gliomas is of particular importance from the viewpoint of examining the THz spectroscopy as a prospective tool for the intraoperative neurodiagnosis of tumors.

Table 1. Sample of human brain tissues measured *in vitro*

#	Tissue type	Intraoperative fluorescence diagnosis
1	Intact tissues	–
2	Meningioma, grade I	5-ALA-induced fluorescence of PpIX was observed
3	Glioma, grade IV	5-ALA-induced fluorescence of PpIX was observed
4	Glioma, grade IV	no 5-ALA-induced fluorescence of PpIX was observed

In order to preserve tissues for the THz measurements, we applied the gelatin-embedding.[43] In contrast to other well-known approaches for tissue fixation (paraffin embedding,[39,52] formalin fixation,[53] freezing,[26,54] and dehydration[55]) the gelatin embedding allows for preventing hydration/dehydration of tissues and, thus, sustaining the water content in tissues and their THz response close to that of freshly-excised ones for a long time after the surgical resection. The gelatin embedding makes the THz measurement *in vitro* similar to that *in vivo*, which is of high importance for analysis of the ability for the intraoperative THz neurodiagnosis. During the transportation and the THz measurements of tissues, they were placed on a reference window and covered with a gelatin slab. After the THz measurements, the tissue specimens were fixed in the formalin and sent to the histological examination, which confirmed the initial diagnosis.

2.2 Experimental setup

For the THz measurements of tissues, we used an experimental setup based on the THz pulsed spectrometer (see Fig. 1 (a)). As an emitter and a detector of the THz pulses, it employs the LT-GaAs photoconductive antennas (PCAs). The antenna emitter is pumped, and the antenna-detector is probed, with the femtosecond laser pulses of the Toptica FErb780 laser. The experimental setup features the maximal spectral operation range of about 0.05 to 4.0 THz and the maximal spectral resolution of about 0.002 THz. It is equipped with the reflection-mode-measurement unit (see Fig. 1 (b)), which is comprised of two off-axis parabolic mirrors for focusing the incident THz beam on the sample surface and collimating the reflected THz beam to the detector, and a reference quartz window for handling the gelatin-embedded tissues sample at the focal point. The THz beam irradiating the sample of interest is s-polarized (an electric field is perpendicular to the plane of incidence). During the measurements, the experimental setup was covered by the plastic housing and purged with the nitrogen gas, which allows for decreasing the humidity along the THz beam path and suppressing an impact of water vapors on the results of the THz measurements. The reference quartz window serves as a part of the housing – it is in contact with the nitrogen atmosphere from the bottom side, and with the air, or the gelatin-embedded tissue sample, from the top side.

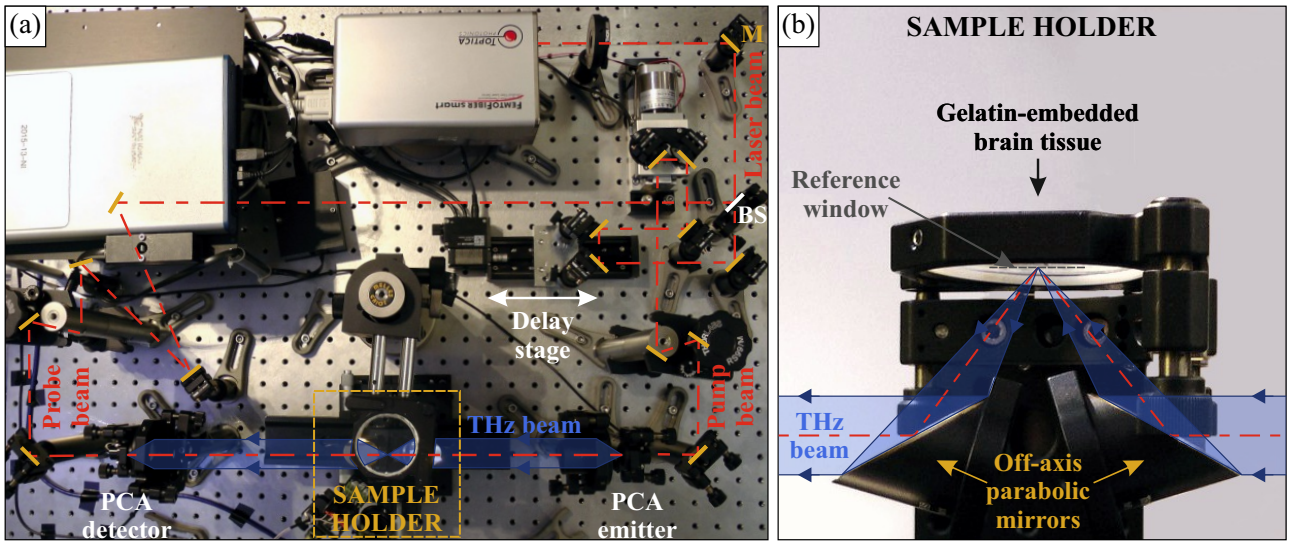

Figure 1. Experimental setup for the *in vitro* THz spectroscopy of the gelatin-embedded human brain tissues: (a) a top view of the experimental setup based on the THz pulsed spectrometer (here, M stands for the flat gold mirror, BS stands for the optical beam splitter); (b) a side view of the reflection-mode-measurement unit, which is comprised of two off-axis parabolic mirrors for the THz beam focusing to, and collimating from, the gelatin-embedded brain tissues placed at the focal point behind a reference quartz window. The plastic housing of the experimental setup and the system of the THz beam path purging with the nitrogen gas are not shown for simplicity.

2.3 The inverse problem solution of the THz pulsed spectroscopy

In order to compare the THz responses of healthy and pathological brain tissues, from the THz measurements, we reconstructed the frequency-dependent refractive index $n(\nu)$ and the amplitude absorption coefficient $\alpha(\nu)$ of biotissues, which are related to the complex refractive index of the sample $\widetilde{n}(\nu)$ as

$$\widetilde{n} = n - i\frac{c}{2\pi\nu}\alpha \tag{1}$$

(here, $c \simeq 3 \times 10^8$ m/s is the speed of light in a free space), do not depend on the method of measurements, and fully describe the THz wave – tissue interactions in the framework of classical electrodynamics.[17]

To reconstruct the refractive index and the amplitude absorption coefficient of tissues, we used the method described in papers.[23,56,57] As shown in Fig. 2, it implies resolving the inverse problem of the THz pulsed spectroscopy relying on processing of the 3 waveforms – i.e. (i) a reference one $E_{\mathrm{r}}(t)$ reflected from the empty window, (ii) a reference one $E_{\mathrm{m}}(t)$ reflected from the window, behind which the flat gold mirror is placed, and (iii) a sample one $E_{\mathrm{s}}(t)$ reflected from the window, behind which the sample of interest is handled. The complex refractive index of the sample ($\widetilde{n} = \widetilde{n}_2$) is reconstructed via the minimization of the error functional

$$\widetilde{n} = \mathrm{argmin}_{\widetilde{n}}\left[\Phi\right], \tag{2}$$

$$\Phi = \left|\widetilde{H}_{\mathrm{exp}} - \widetilde{H}_{\mathrm{th}}\right|^2 + \left|\phi[\widetilde{H}_{\mathrm{exp}}] - \phi[\widetilde{H}_{\mathrm{th}}]\right|^2, \tag{3}$$

where $|...|$ and $\phi[...]$ stand for the modulus and the phase of the complex number, $\widetilde{H}_{\mathrm{exp}}(\nu)$ and $\widetilde{H}_{\mathrm{th}}(\nu, \widetilde{n})$ are the experimental and theoretical transfer functions.

We defined the experimental transfer function based on the measured waveform

$$\widetilde{H}_{\mathrm{exp}} = \frac{\widetilde{E}_{\mathrm{s}} - \widetilde{E}_{\mathrm{r}}}{\widetilde{E}_{\mathrm{m}} - \widetilde{E}_{\mathrm{r}}}, \tag{4}$$

where $\widetilde{E}_{\mathrm{r}}(\nu)$, $\widetilde{E}_{\mathrm{m}}(\nu)$ and $\widetilde{E}_{\mathrm{s}}(\nu)$ stand for the Fourier spectra of the waveforms. The theoretical transfer function assumes interference of all THz pulses presented in the reference and sample waveforms, including the THz pulse reflected from the front surface of the window (see marker I in Fig. 2 (b) and (c)), the THz pulse reflected from the interfaces between the window and the air, the mirror, and the sample (see marker II in Fig. 2 (b) and (c)), and N satellite THz pulses originating from the multiple THz wave reflections within the reference window (for example, see marker III in Fig. 2 (b) and (c), which corresponds to the first satellite pulse)

$$\widetilde{H}_{\mathrm{th}} = \frac{\widetilde{R}_{12} - \widetilde{R}_{10} + \sum_{j=1}^{N}\left(\widetilde{R}_{12}^{j+1} - \widetilde{R}_{10}^{j+1}\right)\widetilde{R}_{10}^{j}\widetilde{P}_1^{2j}}{\widetilde{R}_{13} - \widetilde{R}_{10} + \sum_{j=1}^{N}\left(\widetilde{R}_{13}^{j+1} - \widetilde{R}_{10}^{j+1}\right)\widetilde{R}_{10}^{j}\widetilde{P}_1^{2j}}. \tag{5}$$

$\widetilde{R}_{\mathrm{mk}}(\nu, \widetilde{n}_{\mathrm{m}}, \widetilde{n}_{\mathrm{k}}, \theta_1, \theta_2)$ stands for the Fresnel coefficient of the amplitude reflection from interface between the m^{th} and k^{th} media defined for the s-polarized wave

$$\widetilde{R}_{\mathrm{mk}} = \frac{\widetilde{n}_{\mathrm{m}}\cos\theta_{\mathrm{m}} - \widetilde{n}_{\mathrm{k}}\cos\theta_{\mathrm{k}}}{\widetilde{n}_{\mathrm{m}}\cos\theta_{\mathrm{m}} + \widetilde{n}_{\mathrm{k}}\cos\theta_{\mathrm{k}}}. \tag{6}$$

Here, the indices $\mathrm{m}, \mathrm{k} = 0, 1, 2, 3$ correspond to the air, quartz, tissue and gold mirror, respectively, θ_{m} and θ_{k} stand for the angles of incidence and reflection, which are quite close to the normal incidence. The complex refractive indices of the air $\widetilde{n}_0$ and the quartz $\widetilde{n}_1$, the effective complex refractive index of the gold $\widetilde{n}_3$, and the thickness of the reference window l_1 are known *a priori*. The operator $\widetilde{P}_1(\nu, \widetilde{n}_1, l_1)$ describes the THz wave propagation along the distance $l_1' = l_1/\cos\theta_2$ in the reference quartz window and is defined by the Bouguer-Lambert-Beer law

$$\widetilde{P}_1 = \exp\left(-i\frac{2\pi\nu}{c}\widetilde{n}_1 l_1'\right). \tag{7}$$

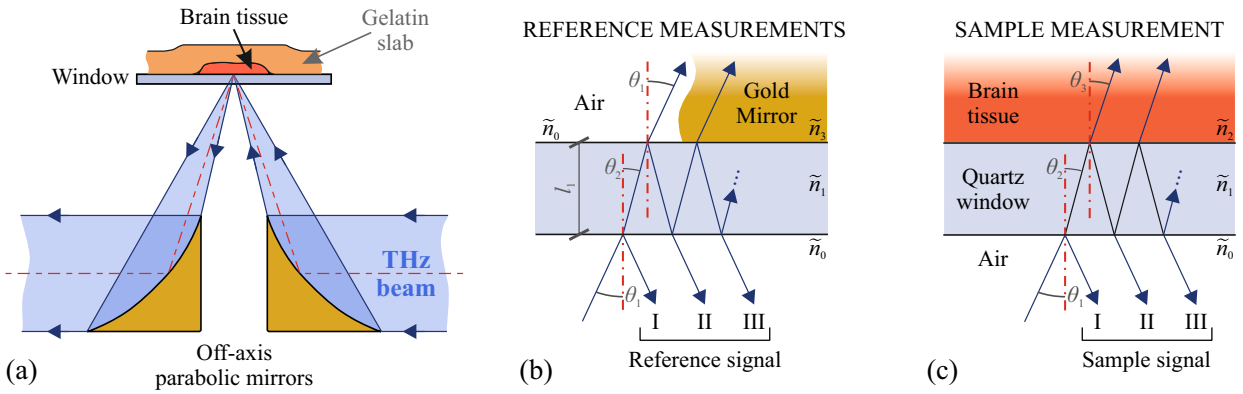

Figure 2. Detection of the reference and sample waveforms using the experimental setup and the reflection-mode-measurement unit: (a) a scheme of the THz beam focusing to, and collimation from, the sample of interest, which is placed behind the reference window; (b) a scheme of the THz wave reflection from the empty reference window, or the reference window with the gold mirror placed behind it, during the detection of the reference waveforms E_{r} and E_{m}, respectively; (c) a scheme of the THz wave reflection from the reference window with the sample of interest handled behind it during the detection of the sample waveform E_{s}. In panels (b) and (c), the characters I, II, and III stand for the separate components of the THz waveforms – i.e. the first THz pulse reflected from the front surface of the reference window, the second THz pulse reflected from the interface between the window and the air, the gold mirror, and the sample, and the third THz pulse (the satellite pulse) originating from the multiple THz wave reflection within the reference window.

3. RESULTS

Figure 3 shows the results of the THz measurements of the gelatin-embedded human brain tissues using the described experimental setup and the method for resolving the inverse problem of the THz pulsed spectroscopy. We reconstructed (a) the refractive index and (b) the amplitude absorption coefficient of 2 malignant gliomas (grade IV), 1 meningioma (grade I), and intact tissue (see Tab. 1) in the frequency range of 0.1 to 1.1 THz. Each tissue sample features a lateral dimensions of about 1.5×1.5 cm^2, which is much larger compared to the size of the THz beam spot. We examined the reproducibility of the experimental data and the fluctuations of the THz response for each tissue specimen by considering different points of its surface – these factors are accounted in the error bars of experimental curves (see Fig. 3).

The observed results demonstrate good reproducibility – i.e. the frequency-dependent curves of the refractive index and the amplitude absorption coefficient are characterized by rather small error bars. In complete agreement with the previous works,[39–42] we observed statistical differences between the THz response of intact tissues and tumors, which might result from the increased water content and the structural changes in tumor tissues. Both meningioma and gliomas possess increased THz refractive index and amplitude absorption coefficient compared to the intact tissues, while the highest statistical differences between the normal and pathological tissues are observed in the frequency range of 0.3 to 0.7 THz. We should particularly notice a contrast between the THz characteristics of the intact tissues and the glioma, for which no 5-ALA-induced fluorescence of PpIX was observed during the intraoperative fluorescence diagnosis (see Tab. 1). This contrast might highlight the potential advantage of the THz diagnosis over the standard methods for the intraoperative diagnosis of brain tumors, the majority of which uses endogenous labels of tumor and features limited sensitivity and specificity.

4. DISCUSSIONS

The use of the gelatin embedding for preserving the tissues makes the THz measurement *in vitro* similar to that *in vivo*, which is important for analysing the ability of the intraoperative THz neurodiagnosis. The results of this preliminary study yield feasibility test, which aims to objectively uncover strengths and weaknesses of the THz spectroscopy from the viewpoint of its use for differentiation between the normal (intact) tissues and the tumors of the brain. They allow us for demonstrating the prospective of the THz technology in the intraoperative neurodiagnosis.

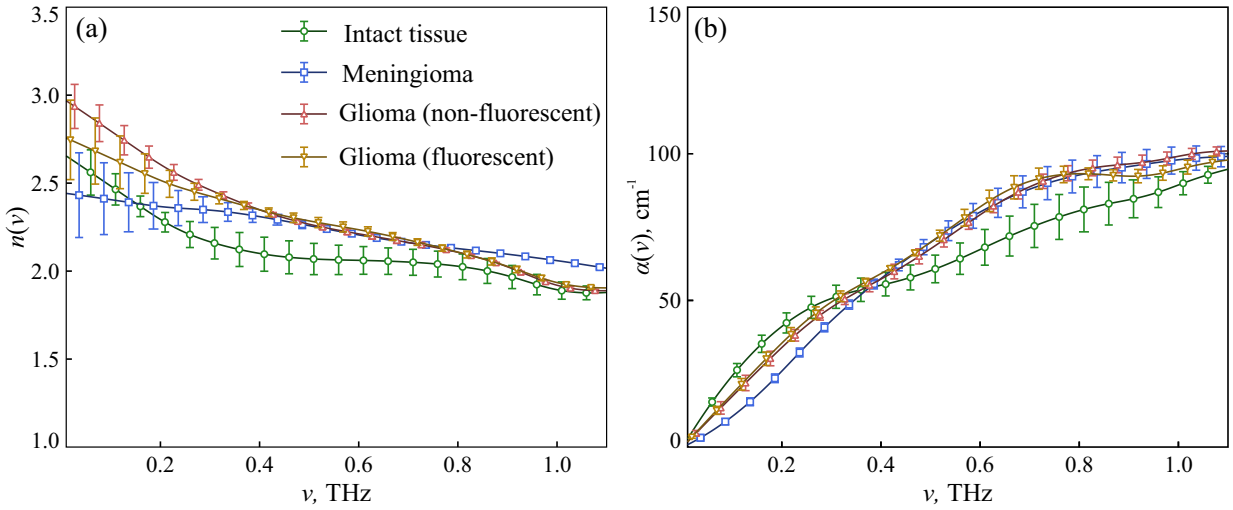

Figure 3. Results of the *in vitro* THz spectroscopy of the gelatin-embedded brain tissues – healthy (intact) tissue, 1 meningioma and 2 gliomas, (one of which fluorescent and non-fluorescent in the presence of 5-ALA): (a) refractive index; (b) amplitude absorption coefficient.

Despite the promising results of the previous[39–42] studies and the recent work, the intraoperative THz neurodiagnosis of brain tumors is still far from practical realization. In order to develop the methods of THz neurodiagnosis and to bring them to a clinical practice, in our future work, we would focus our research efforts on

- Accumulating the verified database of the THz dielectric responses of normal tissues and tumors of the brain;
- Analyzing this database to study an ability for the differentiation between normal and pathological tissues of the brain;
- Selecting the optimal THz frequencies and principal components for the differentiation of healthy tissues and tumors of the brain;
- Estimating the sensitivity and specificity of the THz neurodiagnosis of tumors and comparing the THz methods with other modern modalities of the intraoperative neurodiagnosis;
- Developing the novel THz instruments reliable for use in a clinical environment.

5. CONCLUSIONS

In this paper, we have demonstrated the results of *in vitro* THz spectroscopy of the gelatin-embedded human brain tumors – 2 samples of malignant glioma (grade IV), 1 sample of meningioma (grade I), and samples of intact tissue. By applying the gelatin embedding, we have preserved tissues from hydration/dehydration and sustained their THz response unaltered compared to the freshly-excised tissues for a long time after resection. We have experimentally demonstrated increased refractive index and absorption coefficient of the gelatin-embedded human brain tumors compared to the intact tissues in the THz range of electromagnetic spectrum. The results of this study justify the potential of the THz technology in the intraoperative neurodiagnosis of tumors.

ACKNOWLEDGMENTS

Gelatin embedding, THz measurements, and histological examinations of tissues, performed by N.V. Chernomyrdin, A.A. Gavdush, S.T. Beshplav and K.I. Zaytsev, were supported by the Grant from the Russian Science Foundation (RSF), Project # 17-79-20346. The work of V.V. Tuchin dedicated to the analysis of the data of THz measurements was supported by the Ministry of Education and Science of the Russian Federation, Grant # 17.1223.2017/AP.

REFERENCES

[1] Lee, Y.-S., [*Principles of Terahertz Science and Technology*], Springer, New York, NY, USA (2009).

[2] Popovic, Z. and Grossman, E., "THz metrology and instrumentation," *IEEE Transactions on Terahertz Science and Technology* **1**(1), 133–144 (2011).

[3] Ulbricht, R., Hendry, E., Shan, J., Heinz, T., and Bonn, M., "Carrier dynamics in semiconductors studied with time-resolved terahertz spectroscopy," *Reviews of Modern Physics* **83**(2), 543–586 (2011).

[4] Buron, J., Petersen, D., Boggild, P., Cooke, D., Hilke, M., Sun, J., Whiteway, E., Nielsen, P., Hansen, O., Yurgens, A., and Jepsen, P., "Graphene conductance uniformity mapping," *Nano Letters* **12**(10), 5074–5081 (2012).

[5] Komandin, G., Zhukova, E., Torgashev, V., Boris, A., Boris, A., Motovilova, E., Prokhorov, A., Kadyrov, L., Gorshunov, B., and Dressel, M., "Terahertz-infrared spectra of the rare-earth scandate DyScO3 single crystal," *Journal of Applied Physics* **114**(2), 024102 (2013).

[6] Komandin, G., Chuchupal, S., Lebedev, S., Goncharov, Y., Korolev, A., Porodinkov, O., Spektor, I., and Volkov, A., "BWO generators for terahertz dielectric measurements," *IEEE Transactions on Terahertz Science and Technology* **3**(4), 440–444 (2013).

[7] Jacobsen, R., Mittleman, D., and Nuss, M., "Chemical recognition of gases and gas mixtures with terahertz waves," *Optics Letters* **21**(24), 2011–2013 (1996).

[8] Walther, M., Fischer, B. M., Ortner, A., Bitzer, A., Thoman, A., and Helm, H., "Chemical sensing and imaging with pulsed terahertz radiation," *Analytical and Bioanalytical Chemistry* **397**, 1009–1017 (2010).

[9] Zeitler, J., Taday, P., Newnham, D., Pepper, M., Gordon, K., and Rades, T., "Terahertz pulsed spectroscopy and imaging in the pharmaceutical setting – a review," *Journal of Pharmacy and Pharmacology* **59**(2), 209–223 (2007).

[10] Kawase, K., Ogawa, Y., Watanabe, Y., and Inoue, H., "Non-destructive terahertz imaging of illicit drugs using spectral fingerprints," *Optics Express* **11**(20), 2549–2554 (2003).

[11] Ahi, K., "Mathematical modeling of THz point spread function and simulation of THz imaging systems," *IEEE Transactions on Terahertz Science and Technology* **7**(6), 747–754 (2017).

[12] Grossman, E., Dietlein, C., Ala-Laurinaho, J., Leivo, M., Gronberg, L., Gronholm, M., Lappalainen, P., Rautiainen, A., Tamminen, A., and Luukanen, A., "Passive terahertz camera for standoff security screening," *Applied Optics* **49**(19), E106–E120 (2010).

[13] Dolganova, I., Zaytsev, K., Metelkina, A., Karasik, V., and Yurchenko, S., "A hybrid continuous-wave terahertz imaging system," *Review of Scientific Instruments* **86**(11), 113704 (2015).

[14] Sun, Q., He, Y., Liu, K., Fan, S., Parrott, E., and Pickwell-MacPherson, E., "Recent advances in terahertz technology for biomedical applications," *Quantitative Imaging in Medicine and Surgery* **7**(3), 345–355 (2017).

[15] Yang, X., Zhao, X., Yang, K., Liu, Y., Liu, Y., Fu, W., and Luo, Y., "Biomedical applications of terahertz spectroscopy and imaging," *Trends in Biotechnology* **34**(10), 810–824 (2016).

[16] Berry, E., Walker, G., Fitzgerald, A., Zinov'ev, N., Chamberlain, M., Smye, S., Miles, R., and Smith, M., "Do *in vivo* terahertz imaging systems comply with safety guidelines?," *Journal of Laser Applications* **15**(3), 192–198 (2003).

[17] Pickwell, E., Cole, B., Fitzgerald, A., Wallace, V., and Pepper, M., "Simulation of terahertz pulse propagation in biological systems," *Applied Physics Letters* **84**(12), 2190–192 (2004).

[18] Chen, H., Chen, T.-H., Tseng, T.-F., Lu, J.-T., Kuo, C.-C., Fu, S.-C., Lee, W.-J., Tsai, Y.-F., Huan, Y.-Y., Chuang, E., Hwang, Y.-J., and Sun, C.-K., "High-sensitivity *in vivo* THz transmission imaging of early human breast cancer in a subcutaneous xenograft mouse model," *Optics Express* **19**(22), 21552–21562 (2011).

[19] Yamaguchi, S., Fukushi, Y., Kubota, O., Itsuji, T., Ouchi, T., and Yamamoto, S., "Origin and quantification of differences between normal and tumor tissues observed by terahertz spectroscopy," *Physics in Medicine and Biology* **61**(18), 6808–6820 (2016).

[20] Woodward, R., Wallace, V., Pye, R., Cole, B., Arnone, D., Linfield, E., and Peppern, M., "Terahertz pulse imaging of *ex vivo* basal cell carcinoma," *Journal of Investigative Dermatology* **120**(1), 72–78 (2003).

[21] Wallace, V., Fitzgerald, A., Hankar, S., Lanagan, N., Pye, R., Cluff, J., and Arnone, D., "Terahertz pulsed imaging of basal cell carcinoma *ex vivo* and *in vivo*," *British Journal of Dermatology* **151**(2), 424–432 (2004).

[22] Joseph, C., Patel, R., Neel, V., Giles, R., and Yaroslavsky, A., "Imaging of *ex vivo* nonmelanoma skin cancers in the optical and terahertz spectral regions. Optical and terahertz skin cancers imaging," *Journal of Biophotonics* **7**(5), 295–303 (2014).

[23] Zaytsev, K., Kudrin, K., Karasik, V., Reshetov, I., and Yurchenko, S., "*In vivo* terahertz spectroscopy of pigmentary skin nevi: Pilot study of non-invasive early diagnosis of dysplasia," *Applied Physics Letters* **106**(5), 053702 (2015).

[24] Truong, B., Tuan, H., Wallace, V., Fitzgerald, A., and Nguyen, H., "The potential of the double Debye parameters to discriminate between basal cell carcinoma and normal skin," *IEEE Transactions on Terahertz Science and Technology* **5**(6), 990–998 (2015).

[25] Reid, C., Fitzgerald, A., Reese, G., Goldin, R., Tekkis, P., O'Kelly, P., Pickwell-MacPherson, E., Gibson, A., and Wallace, V., "Terahertz pulsed imaging of freshly excised human colonic tissues," *Physics in Medicine and Biology* **56**(14), 4333–4353 (2011).

[26] Sim, Y., Park, J., Ahn, K.-M., Park, C., and Son, J.-H., "Terahertz imaging of excised oral cancer at frozen temperature," *Biomedical Optics Express* **4**(8), 1413–1421 (2013).

[27] Eadie, L.H., Reid, C.B., Fitzgerald, A.J., Wallace, V.P., "Optimizing multi-dimensional terahertz imaging analysis for colon cancer diagnosis," *Expert Systems with Applications* **40**(6), 0957–4174 (2013).

[28] Hua, C., Shi-Hua, M., Wen-Xing, Y., Xiu-Mei, W., and Xiao-Zhou, W., "The diagnosis of human liver cancer by using THz fiber-scanning near-field imaging," *Chinese Physics Letters* **30**(3), 030702 (2013).

[29] Hou, D., Li, X., Cai, J., Ma, Y., Kang, X., Huang, P., and Zhang, G., "Terahertz spectroscopic investigation of human gastric normal and tumor tissues," *Physics in Medicine and Biology* **59**(18), 5423–5440 (2014).

[30] Ji, Y., Park, C., Kim, H., Kim, S.-H., Lee, G., Noh, S., Jeon, T.-I., Son, J.-H., Huh, Y.-M., Haam, S., Oh, S., Lee, S., and Suh, J.-S., "Feasibility of terahertz reflectometry for discrimination of human early gastric cancers," *Biomedical Optics Express* **6**(4), 1398–1406 (2015).

[31] Wahaia, F., Kasalynas, I., Venckevicius, R., Seliuta, R., Valusis, G., Urbanowicz, A., Molis, G., Carneiro, F., Carvalho Silva, C., and Granja, P., "Terahertz absorption and reflection imaging of carcinoma-affected colon tissues embedded in paraffin," *Journal of Molecular Structure* **1107**, 214–219 (2016).

[32] Fitzgerald, A., Wallace, V., Jimenez-Linan, M., Bobrow, L., Pye, R., Purushotham, A., and Arnone, D., "Terahertz pulsed imaging of human breast tumors," *Radiology* **239**(2), 533–540 (2006).

[33] Ashworth, P., Pickwell-MacPherson, E., Provenzano, E., Pinder, S., Purushotham, A., Pepper, M., and Wallace, V., "Terahertz pulsed spectroscopy of freshly excised human breast cancer," *Optics Express* **17**(15), 12444–12454 (2009).

[34] Fitzgerald, A., Wallace, V., Pinder, S., Purushotham, A., O'Kelly, P., and Ashworth, P., "Classification of terahertz-pulsed imaging data from excised breast tissue," *Journal of Biomedical Optics* **17**(1), 016005 (2012).

[35] Fitzgerald, A., Pickwell-MacPherson, E., and Wallace, V., "Use of finite difference time domain simulations and Debye theory for modelling the terahertz reflection response of normal and tumour breast tissue," *PLOS ONE* **9**, 1–9 (2014).

[36] Truong, B., Tuan, H., Fitzgerald, A., Wallace, V., and Nguyen, H., "A dielectric model of human breast tissue in terahertz regime," *IEEE Transactions on Biomedical Engineering* **62**(2), 699–707 (2015).

[37] Wilmink, G.J., Ibey, B.L., Tongue, T., Schulkin, B., Laman, N., Peralta, X.G., Roth, C.C., Cerna, C.Z., Rivest, B.D., Grundt, J.E., Roach, W.P., "Development of a compact terahertz time-domain spectrometer for the measurement of the optical properties of biological tissues," *Journal of Biomedical Optics* **16**(4), 047006 (2011).

[38] Grootendorst, M., Fitzgerald, A.J., Brouwer de Koning, S., Santaolalla, A., Portieri, A., Van Hemelrijck, M., Young, M., Owen, J., Cariati, M., Pepper, M., Wallace, V., Pinder, S., and Purushotham, A., "Use of a handheld terahertz pulsed imaging device to differentiate benign and malignant breast tissue," *Biomedical Optics Express* **8**(6), 2932–2945 (2017).

[39] Meng, K., Chen, T.-N., Chen, T., Zhu, L.-G., Liu, Q., Li, Z., Li, F., Zhong, S.-C., Li, Z.-R., Feng, H., and Zhao, J.-H., "Terahertz pulsed spectroscopy of paraffin-embedded brain glioma," *Journal of Biomedical Optics* **19**(7), 077001 (2014).

[40] Oh, S., Kim, S.-H., Ji, Y., Jeong, K., Park, Y., Yang, J., Park, D., Noh, S., Kang, S.-G., Huh, Y.-M., Son, J.-H., and Suh, J.-S., "Study of freshly excised brain tissues using terahertz imaging," *Biomedical Optics Express* **5**(8), 2837–2842 (2014).

[41] Yamaguchi, S., Fukushi, Y., Kubota, O., Itsuji, T., Ouchi, T., and Yamamoto, S., "Brain tumor imaging of rat fresh tissue using terahertz spectroscopy," *Scientific Reports* **6**, 30124 (2016).

[42] Ji, Y., Oh, S., Kang, S.-G., Heo, J., Kim, S.-H., Choi, Y., Song, S., Son, H., Kim, S., Lee, J., Haam, S., Huh, Y., Chang, J., Joo, C., and Suh, J.-S., "Terahertz reflectometry imaging for low and high grade gliomas," *Scientific Reports* **6**, 36040 (2016).

[43] Fan, S., Ung, B., Parrott, E., and Pickwell-MacPherson, E., "Gelatin embedding: a novel way to preserve biological samples for terahertz imaging and spectroscopy," *Physics in Medicine and Biology* **60**(7), 2703–2713 (2015).

[44] Tuchin, V., [*Tissue Optics: Light Scattering Methods and Instruments for Medical Diagnosis: Third Edition*], SPIE (2015).

[45] Tuchin, V., "Tissue optics and photonics: Biological tissue structures," *Journal of Biomedical Photonics and Engineering* **1**(1), 3–21 (2015).

[46] Tuchin, V., "Tissue optics and photonics: Light-tissue interaction," *Journal of Biomedical Photonics and Engineering* **1**(2), 2469 (2015).

[47] Tuchin, V., "Tissue optics and photonics: Light-tissue interaction II," *Journal of Biomedical Photonics and Engineering* **2**(3), 030201 (2016).

[48] Potapov, A., Goryaynov, S., Okhlopkov, V., Shishkina, L., Loschenov, V., Savelieva, T., Golbin, D., Chumakova, A., Goldberg, M., Varyukhina, M., and Spallone, A., "Laser biospectroscopy and 5-ALA fluorescence navigation as a helpful tool in the meningioma resection," *Neurosurgical Review* **39**(3), 437–447 (2016).

[49] Pustogarov, N., Panteleev, D., Goryaynov, S., Ryabova, A., Rybalkina, E., Revishchin, A., Potapov, A., and Pavlova, G., "Hiding in the shadows: CPOX expression and 5-ALA induced fluorescence in human glioma cells," *Molecular Neurobiology* **54**(7), 5699–5708 (2017).

[50] Shikunova, I., Stryukov, D., Rossolenko, S., Kiselev, A., and Kurlov, V., "Neurosurgery contact handheld probe based on sapphire shaped crystal," *Journal of Crystal Growth* **457**, 265–269 (2017).

[51] Shikunova, I., Zaytsev, K., Stryukov, D., Dubyanskaya, E., and Kurlov, V., "Neurosurgical sapphire handheld probe for intraoperative optical diagnostics, laser coagulation and aspiration of malignant brain tissue," *Proceedings of SPIE* **10411**, 104110Q (2017).

[52] Formanek, F., Brun, M.-A., and Yasuda, A., "Contrast improvement of terahertz images of thin histopathologic sections," *Biomedical Optics Express* **2**(1), 58–64 (2011).

[53] Sun, Y., Fischer, B., and Pickwell-MacPherson, E., "Effects of formalin fixing on the terahertz properties of biological tissues," *Journal of Biomedical Optics* **14**(6), 064017 (2009).

[54] He, Y., Ung, N.-Y., Parrott, E., Ahuja, A., and Pickwell-MacPherson, E., "Freeze-thaw hysteresis effects in terahertz imaging of biomedical tissues," *Biomedical Optics Express* **7**(11), 4711–4717 (2016).

[55] He, Y., Liu, K., Au, C., Sun, Q., Parrott, E.P.J., and Pickwell-MacPherson, E., "Determination of terahertz permittivity of dehydrated biological samples," *Physics in Medicine and Biology* **62**(23), 8882–8893 (2017).

[56] Zaytsev, K., Gavdush, A., Chernomyrdin, N., and Yurchenko, S., "Highly accurate *in vivo* terahertz spectroscopy of healthy skin: Variation of refractive index and absorption coefficient along the human body," *IEEE Transactions on Terahertz Science and Technology* **5**(5), 817–827 (2015).

[57] Zaitsev, K., Chernomyrdin, N., Kudrin, K., Reshetov, I., and Yurchenko, S., "Terahertz spectroscopy of pigmentary skin nevi *in vivo*," *Optics and Spectroscopy* **119**(3), 404–410 (2015).